Ferroelectricity in $SrTiO_3$–$BiScO_3$ system

Oleg Ivanov*, Elena Danshina, Yulia Tuchina, and Vyacheslav Sirota

Joint Research Centre "Diagnostics of Structure and Properties of Nanomaterials", Belgorod State University, Pobedy St., 85, 308015 Belgorod, Russia

Keywords ceramics, ferroelectrics, phase transitions, solid solutions

Ceramic solid solutions of the $(1-x)SrTiO_3$–$xBiScO_3$ system with $x = 0$, 0.05, 0.1, 0.2, 0.3, 0.4, and 0.5 were synthesized for the first time via solid-state processing techniques. Both of the end members in this system are not ferroelectric materials. X-ray diffraction analysis revealed that at room temperature the samples with $x = 0.2$, 0.3, and 0.4 consist of mixtures of cubic center-symmetric $Pm3m$ phase and tetragonal polar $P4mm$ phase. Dielectric measurements of these compositions demonstrated anomalies associated with a diffuse ferroelectric phase transition. Furthermore, examination of the polarization hysteresis behavior revealed weakly nonlinear hysteresis loops in the ferroelectric phase.

1 Introduction Strontium titanate, $SrTiO_3$, is known to be an incipient ferroelectric lying near the limit of its paraelectric phase stability [1]. Various impurities substituted for the host ions in $SrTiO_3$ in both the *A*- and *B*-positions can induce either a ferroelectric phase transition or a distinct dielectric relaxation [2–7].

$BiScO_3$ is an interesting end member for fabrication of new ceramic solid solutions [8–10]. Despite its utility in solid solutions, there is little knowledge about the $BiScO_3$ member itself. In particular, it is not known at present whether $BiScO_3$ is ferroelectric. The polar $C2/c$ symmetry of $BiScO_3$ allows us to consider this compound as a potential ferroelectric. However, although by symmetry reasons it has been speculated that $BiScO_3$ may be a ferroelectric material, no experimental confirmations were reported [11].

The $SrTiO_3$–$BiScO_3$ system is a new and attractive system in a family of ceramic solid solutions with $BiScO_3$ as one of the end members.

It is important that at room temperature $SrTiO_3$ has a cubic $Pm3m$ structure, while $BiScO_3$ is a monoclinic $C2/c$ compound. Therefore, a change of symmetry from tetragonal to monoclinic should be observed as the mole fraction of $BiScO_3$ increased. Moreover, taking into account a considerable difference in structures of the end members in the $SrTiO_3$–$BiScO_3$ system, intermediate phases with other symmetries including polar structures may be formed for some compositions.

2 Experimental procedure Solid solutions of $(1-x)SrTiO_3$–$xBiScO_3$ with $x = 0$, 0.05, 0.1, 0.2, 0.3, 0.4, and 0.5 were synthesized via solid-state processing techniques from powders of $SrCO_3$, TiO_2, Bi_2O_3, and Sc_2O_3 taken as starting materials. After preliminary milling and drying, the powders were calcined at 1073 K for 4 h and at 1123 K for 4 h in air atmosphere. The calcined powders were then cold isostatically pressed at 400 MPa. The pressed samples were sintered at 1623 K for 5 h. The weight loss during sintering was confirmed to be less than 1% for all samples. An additional 3 mol% Bi_2O_3 was added as a sintering aid before pressing the samples for compositions with $x = 0$, 0.05, and 0.1. It is known [8] that the excess Bi_2O_3 can improve the densities of the samples during the sintering, because Bi_2O_3 has a melting temperature of about 1100 K, which is lower than the sintering temperatures used in this study. The densities of all samples were higher than 90% of the value of the theoretical density.

X-ray diffraction (XRD) analysis was performed at room temperature for phase determination using a Rigaku Ultima IV diffractometer with Cu Kα radiation. Pellets of 8 mm in diameter and 1 mm in thickness with silver paste as electrodes were prepared for dielectric measurements. The dielectric permittivity ε was measured using a BR2876 LRC meter at a frequency of 1 MHz. A Sawyer–Tower circuit was used to record the polarization versus electric field hysteresis loops.

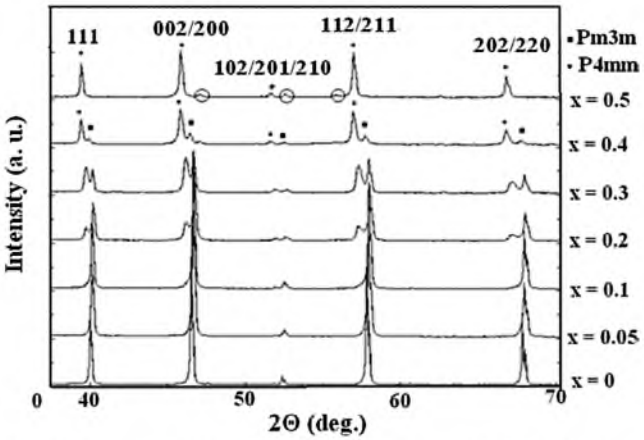

Figure 1 X-ray diffraction patterns of $(1-x)SrTiO_3$–$xBiScO_3$ solid solutions (symbols ○ are corresponding to undesired phases).

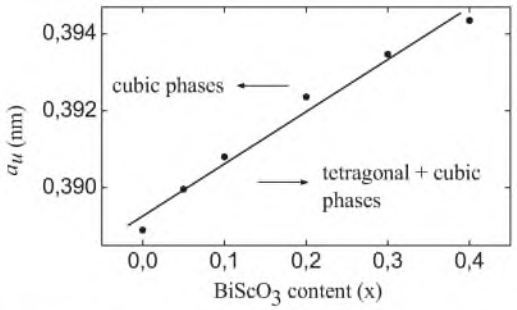

Figure 3 Unit-cell parameter as a function of $BiScO_3$ content.

3 Results Figure 1 displays the XRD patterns for sintered samples of $(1-x)SrTiO_3$–$xBiScO_3$. It should be noted that all of the compositions with $x = 0$–0.5 could be prepared in the perovskite phases with little or no undesired phases. Solid solutions with $x = 0$, 0.05, and 0.1 were found to be corresponding to pure cubic *Pm3m* symmetry. Analysis of the XRD patterns allows us to conclude that the compositions with $x = 0.2$, 0.3, and 0.4 consist of mixtures of cubic *Pm3m* phase and tetragonal *P4mm* phase. Undesired phase peaks were clearly observed for $x = 0.5$. These phases matched the powder diffraction peaks of Bi_2O_3 and Sc_2O_3. The sample with $x = 0.5$ was eliminated from further investigation.

The tetragonal *P4mm* structure is characterized by splitting of the single cubic (210) peak into three diffraction peaks corresponding to the tetragonal (102), (201), and (210) peaks, as is shown in Fig. 2. Additional right-hand-side peaks in Fig. 2 are due to the Cu $K\alpha_2$ radiation.

The methods of Savitzky and Golay [12] and Sonneveld and Visser [13] were applied to analyze the XRD patterns. The lattice parameters were determined for at least six or four indexed diffraction peaks for tetragonal and cubic phases, respectively. Tetragonal structures for $x \geq 0.2$ can be formally reduced to cubic structures with unit-cell parameter calculated as $a_r = (a^2 b)^{1/3}$, where a and b are tetragonal cell

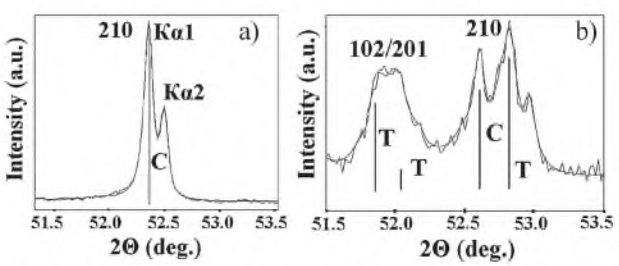

Figure 2 Enlarged part of diffraction peak in the range of $2\theta = 51.5$–53.5 for the samples with $x = 0$ (a) and $x = 0.3$ (b). C: cubic phase and T: tetragonal phase.

parameters derived experimentally [14]. Figure 3 shows the unit-cell parameter, a_u, for the solid solution under study, where $a_u = a_r$ for compositions with $x \geq 0.2$ and a_u is equal to the parameter of the true cubic cell for solid solutions with $x = 0$, 0.05, and 0.1. The linear increase in the a_u parameter with $BiScO_3$ content is consistent with Vegard's law, confirming a solid solution.

Therefore, according to our XRD data, cubic center-symmetric *Pm3m* phase and tetragonal polar *P4mm* phase are coexisting in the samples with $x = 0.2$, 0.3, and 0.4. Such a kind of phase coexistence in some temperature range is one of the specific signs of the ferroelectrics with a diffuse phase transition (or relaxor ferroelectrics). It is known that a ferroelectric diffuse phase transition is accompanied by anomalous behavior of dielectric properties [15]. Figure 4a shows the dielectric permittivity ε versus temperature T for the samples with $x = 0.2$, 0.3, and 0.4. Broad peaks of ε are observed in the T dependences for these compositions.

It was found that the maximum of the dielectric permittivity, ε_m, and the temperature of the $\varepsilon(T)$ peaks, T_m, increased with increasing $BiScO_3$ content. For ferroelectrics with a sharp phase transition the temperature dependence of ε for the high-temperature part of the $\varepsilon(T)$ peak obeys the Curie–Weiss law. In this case the dependence of $1/\varepsilon$ versus temperature (or the temperature difference $(T - T_m)$) should be linear and the slope of this line can be used to estimate the Curie–Weiss constant, C_{CW}. Figure 4b shows that the experimental $\varepsilon(T)$ curves start to deviate from the Curie–Weiss behavior just below temperature T_d. This feature can be taken as evidence of diffusing of the phase transition under study. The temperature T_d called the Burns temperature is corresponding to the appearance of polar nanoregions inside a non-polar matrix during the diffuse phase transition [16].

For a diffuse phase transition, the $\varepsilon(T)$ dependence between T_d and T_m can be fitted by the expression [15]

$$\frac{\varepsilon_m}{\varepsilon(T)} = 1 + \frac{(T - T_m)^\gamma}{2\sigma^2} \tag{1}$$

where σ is the degree of diffuseness of the phase transition and γ is the degree of dielectric relaxation. For a sharp ferroelectric phase transition $\gamma = 1$ and consequent diffusing

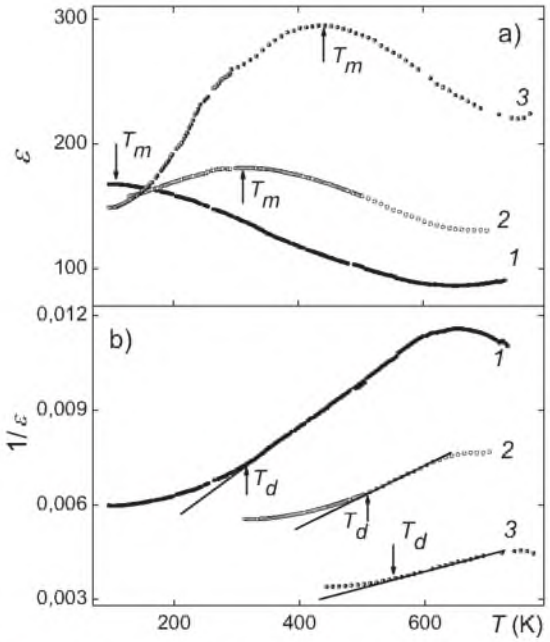

Figure 4 Temperature dependences of ε and $1/\varepsilon$ for $(1-x)SrTiO_3$–$xBiScO_3$ solid solutions: (1) $x=0.2$, (2) $x=0.3$, and (3) $x=0.4$.

of the phase transition leads to γ increasing up to 2 in that larger values of γ express more relaxor behavior of the ferroelectric. Figure 5 shows the dependence of $\ln[(\varepsilon_m/\varepsilon)-1]$ versus $\ln(T-T_m)$ for compositions with $x=0.2$ and 0.3.

One can see that the expression (1) reproduces the experimental data very well. To make this figure more detailed, such a dependence for the sample with $x=0.4$ was eliminated. Both γ and σ were determined from the slope and intercept of lines in Fig. 5. It is known that relaxor

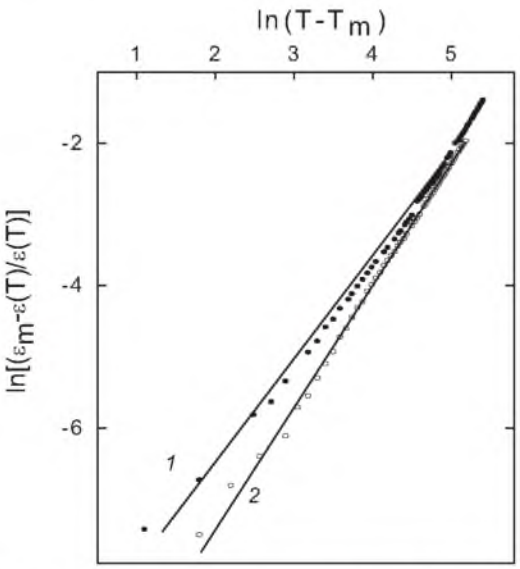

Figure 5 Dependences of of $\ln[(\varepsilon_m/\varepsilon)-1]$ versus $\ln(T-T_m)$ for $(1-x)SrTiO_3$–$xBiScO_3$ solid solutions: (1) $x=0.2$ and (2) $x=0.3$.

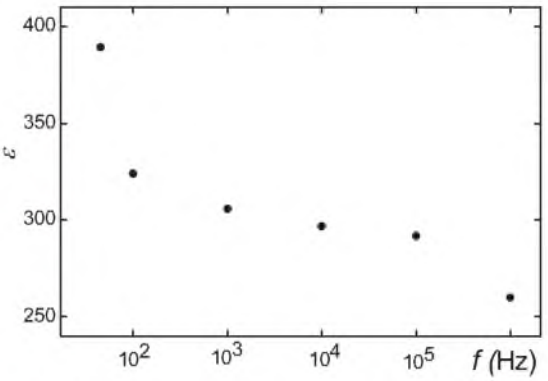

Figure 6 Frequency dependence of dielectric permittivity for the sample with $x=0.4$.

ferroelectrics are characterized by strong frequency dependence of dielectric properties in the relaxor state. A detailed study of the frequency dispersion of dielectric properties of ceramic solid solutions of the $(1-x)SrTiO_3$–$xBiScO_3$ system is in progress. However, a preliminary study allowed us to find the frequency dependence of the dielectric permittivity of the samples under study, as is shown as an example for the sample with $x=0.4$ in Fig. 6 (data taken at room temperature).

Dielectric properties and characteristics of the diffuse phase transition for the compositions with $x=0.2$, 0.3, and 0.4 are listed in Table 1. According to the table, a greater percentage of $BiScO_3$ resulted in a higher degree of diffuseness and a stronger relaxor behavior. This can be explained by the increased cation disorder due to the substitution on the *A*-site by Bi and on the *B*-site by Sc in the $SrTiO_3$ structure.

In order to confirm a ferroelectric nature of the diffuse phase transition, polarization versus electric field measurements at 50 Hz were performed for the samples under study.

Weakly nonlinear hysteresis loops of ferroelectric type were observed at room temperature, as is shown in the inset of Fig. 7 for the composition $x=0.4$.

4 Discussion It is known [2–7] that divalent ions substituting for Sr^{2+} in the *A*-position (Ca^{2+}, Pb^{2+}, and Cd^{2+}) can destroy the stability of the paraelectric state of $SrTiO_3$ and induce a ferroelectric phase transition with critical concentration of impurity at $x_c=0.002$. This concentration is almost the same for all these impurities. Isovalent impurities in the *B*-position (Zr^{4+}, Sn^{4+}, and Ge^{4+})

Table 1 Dielectric data and characteristics of the diffuse phase transition for $(1-x)SrTiO_3$–$xBiScO_3$.

x	T_m (K)	ε_m	C_{CW} (10^4 K)	T_d (K)	σ (K)	γ
0.2	100	167	6.84	320	105	1.58
0.3	312	180	10.42	505	149	1.71
0.4	443	295	19.08	570	173	1.95

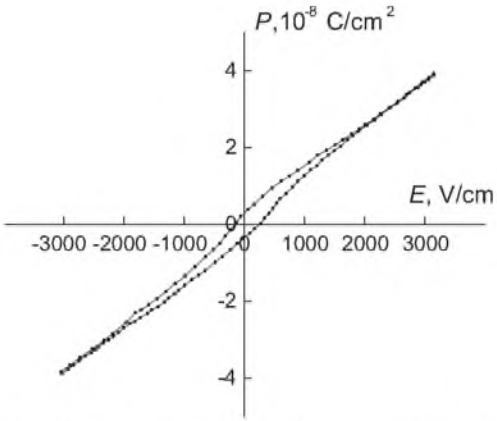

Figure 7 Hysteresis loop for the composition with $x = 0.4$.

have a much smaller effect on dielectric properties of $SrTiO_3$. Instead of an induced ferroelectric phase transition, a distinct dielectric relaxation is observed in $SrTiO_3$ with heterovalent impurities. In particular, a few relaxation processes were found for Bi:$SrTiO_3$ [5–7]. These processes can be interpreted by Skanavi's model [7]. Skanavi's model describes the small motion of Ti^{4+} ions in six equivalent potential minima, which caused the reorientation of the dipoles, and contributed to the dielectric relaxation. In the framework of another model, dielectric relaxation in Bi:$SrTiO_3$ is believed to be closely related to the oxygen vacancies [5].

Simultaneous substitution of the host Sr^{2+} and Ti^{4+} ions by impurity ions by fabrication of solid solutions gives some specific effects. For example, in $SrTiO_3$–$PbMg_{1/3}Nb_{2/3}O_3$ the diffuse ferroelectric phase transition was observed only at $x > 0.2$ with a linear dependence of the transition temperature on composition, which was associated with random fields due to disordered Mg^{2+} and Nb^{5+} distributions [4].

Peculiarities of properties of the $SrTiO_3$–$BiScO_3$ system found in our research are similar to the same peculiarities of the $SrTiO_3$–$PbMg_{1/3}Nb_{2/3}O_3$ system and can be attributed to the diffuse ferroelectric phase transition. But, in contrast with the $SrTiO_3$–$PbMg_{1/3}Nb_{2/3}O_3$ system where $PbMg_{1/3}Nb_{2/3}O_3$ is a relaxor ferroelectric, in $SrTiO_3$–$BiScO_3$ both of the end members are not ferroelectrics.

It is also known that in other solid solutions containing $BiScO_3$ as one of the end members ($BaTiO_3$–$BiScO_3$ [8] and $PbTiO_3$–$BiScO_3$ [9, 10]), significant changes of crystal structure of solid solutions, phase coexistence and diffusing of the ferroelectric phase transition have been found. However, in these systems again non-ferroelectric $BiScO_3$ effects on properties of the ferroelectric member of a system ($BaTiO_3$ or $PbTiO_3$) like $SrTiO_3$ changes the ferroelectric properties of $PbMg_{1/3}Nb_{2/3}O_3$.

It should be finally noted that no dielectric relaxation typical for Bi:$SrTiO_3$ was found in our research for the temperature range under study.

5 Conclusion Ceramic solid solutions of the $(1-x)SrTiO_3$–$xBiScO_3$ system with $x = 0$, 0.05, 0.1, 0.2, 0.3, 0.4, and 0.5 were synthesized for the first time. The end members in this system are not ferroelectrics. XRD analysis revealed that at room temperature the compositions with $x = 0.2$, 0.3, and 0.4 consist of mixtures of cubic center-symmetric $Pm3m$ phase and tetragonal polar $P4mm$ phase. Dielectric anomalies associated with a diffuse ferroelectric phase transition were found for these compositions. The relaxor ferroelectric behavior was likely due to complex processes of cation substitution and ordering on the A-site and on the B-site.

Acknowledgements This work was performed in the framework of the federal target program "Scientific and Pedagogical Staff for Innovative Russia" for 2009–2013 under Contract No. P415.

References

[1] K. A. Muller, Phys. Rev. B **19**, 3593 (1973).
[2] V. V. Lemanov, E. P. Smirnova, P. P. Syrnikov, and E. A. Tarakanov, Phys. Rev. B **54**, 3151 (1996).
[3] V. V. Lemanov, A. V. Sotnikov, E. P. Smirnova, and M. Weihnacht, Fiz. Tverd. Tela **44**, 32 (2002).
[4] V. V. Lemanov, A. V. Sotnikov, E. P. Smirnova, M. Weihnacht, and W. Haßler, Fiz. Tverd. Tela **41**, 1091 (1999).
[5] C. Ang, Z. Yu, and L. E. Cross, Phys. Rev. B **62**, 228 (2000).
[6] C. Ang, Z. Yu, J. Hemberger, and A. Loidl, Phys. Rev. B **59**, 6670 (1999).
[7] G. I. Skanavi and V. A. Matveeva, Zh. Eksp. Teor. Fiz. **30**, 1047 (1956).
[8] H. Ogihara, C. A. Randall, and S. Trolier-McKinstry, J. Am. Ceram. Soc. **92**, 110 (2009).
[9] R. E. Eitel, S. J. Zhang, T. R. Shrout, and C. A. Randall, J. Appl. Phys. **96**, 2828 (2004).
[10] R. E. Eitel, C. A. Randall, T. A. Shrout, and S.-E. Park, J. Soc. Appl. Phys. **41**, 2009 (2002).
[11] S. Trolier-McKinstry, M. D. Biegalski, J. Wang, A. A. Belik, E. Takayama-Muromachi, and I. Levin, J. Appl. Phys. **104**, 044102 (2008).
[12] A. Savitzky and M. J. E. Golay, Anal. Chem. **36**, 1627 (1964).
[13] E. J. Sonneveld and J. W. Visser, J. Appl. Crystallogr. **8**, 12 (1975).
[14] N. V. Zaitsev, E. P. Smirnova, and V. V. Lemanov, Fiz. Tverd. Tela **49**, 488 (2007).
[15] C.-C. Huang, D. P. Cann, X. Tan, and N. Vittayakorn, J. Appl. Phys. **102**, 044103 (2007).
[16] G. Burns and F. H. Dacol, Phys. Rev. B **28**, 2527 (1983).